

## Preferentially regulated expression of connexin 43 in the developing spiral ganglion neurons and afferent terminals in post-natal rat cochlea

W.J. Liu, J. Yang

Department of Otorhinolaryngology-Head & Neck Surgery, Xinhua Hospital, Shanghai Jiaotong University School of Medicine, Shanghai Jiaotong University School of Medicine Ear Institute, Shanghai Key Laboratory of Translational Medicine on Ear and Nose diseases, Shanghai, China

### Abstract

The expression pattern of connexin 43 (Cx43) in the cochlea is not determined and is controversial. Since the presence of Cx43 is essential for hearing, we re-examined its distribution during post-natal development of rat cochlea. Cx43 protein was expressed in spiral ganglion neurons (SGNs) and their neurite terminals innervating the inner and outer hair cells (IHCs and OHCs) as early as birth (post-natal day 0, P0), and persisted until P14. Double immunofluorescence staining, using two antibodies against Cx43 and TUJ1, a marker for all SGNs and afferent terminals, showed that immunoreactivity for Cx43 and TUJ1 was perfectly colocalized in SGNs and afferent terminals associated with the IHCs and OHCs. However, beyond P14, Cx43 immunostaining could no longer be detected in the region of the synaptic terminals at the bases of IHCs and OHCs (P17, adult). In contrast, Cx43 maintained its expression in SGNs into adulthood. We further performed quantitative real-time reverse transcription polymerase chain reaction (qRT-PCR) to identify the presence of Cx43 mRNA in the modiolus (mainly containing SGNs). Cx43 mRNA was higher at P8, compared with P1, and subsequently decreased at P14. These results indicated that Cx43 correlated with cochlear synaptogenesis and establishment of auditory neurotransmission.

### Introduction

Intercellular channels that connect the cytoplasm of contiguous cells are formed by gap junctions (GJs) that consist of a pair of hemichannels, termed connexons. Each hemichannel is comprised of six connexins.<sup>1,2</sup> The importance of connexins in hearing has been established. Mutations in some connexin proteins, such as

connexin 26 (Cx26), Cx30, and Cx43, can cause non-syndromic deafness,<sup>3-5</sup> accounting for 70-80% in newborns,<sup>6</sup> however, the mechanism underlying deafness has not been recognized. The supporting cells in the cochlea form intercellular networks coupled through GJ channels by which the transfer of ions, metabolites and second messengers between cells are mediated.<sup>7</sup> Moreover, it has been proposed that the hair cells receive nutrient and energy supplies from the supporting cells by means of mediators released through hemichannels.<sup>8</sup> Thus, connexin mutation is likely to interfere the vital cochlear signaling function and the possible nutrient supply to the hair cells, in turn, leading to deafness.

In addition, the temporal-spatial distribution of Cx26 in the embryonic and early postnatal rat cochlea suggested that GJ channels play essential roles in cochlear postnatal development and maturation.<sup>9,10</sup> Thus, a detailed description of the expression patterns of these connexin proteins in the developing cochlea can provide important clues for the mechanisms of Cx-related hearing loss. The distribution and expression of Cx26 and Cx30 in the cochlea have been well documented;<sup>11</sup> however, the precise localization of Cx43 in the cochlea remains unknown and is controversial. For example, Cohen-Salmon *et al.* used X-gal staining from Cx43 knockout mice to examine the localization of Cx43.<sup>12</sup> They found that Cx43 expression was restricted to the bone of the otic capsule from post-natal day 8 (P8) onward. Of particular interest was the X-gal staining pattern, which mirrored endogenous Cx43 expression, and was found in the modiolus during the early stages of rat cochlear development. Unfortunately, since nuclear X-gal staining made the visualization of morphologically identifiable cells difficult, Cx43 expression was overlooked in less detailed analyses. Furthermore, the authors explained that the differences between their results and previous immunohistochemistry results were attributed to decalcification of the preparations in the adult inner ear. Recently, Kim *et al.* found only minimal presence of Cx43 in the organ of Corti.<sup>13</sup> However, the implication of the data seems to be unclear because of the lower resolution and quality of their figures. Suzuki *et al.* detected distribution of Cx43 in surface preparations of the adult rat.<sup>14</sup> They showed a small number of tiny, round, particulate, and separate Cx43 immunostaining patterns in the *stria vascularis*, spiral ligament, spiral limbus, and between the adjacent supporting cells of the organ of Corti; however, these observations cannot explain the role of Cx43 in the cochlea. One possible explanation for these contradictory results is that the pattern of connexin staining depends on tissue fixation conditions, including fixative solution, fixation strength, and post-fixation time.<sup>15</sup> Nagy *et al.* proposed that the post-fixation step was essential because post-fixation for 2 h led to almost the entire loss of immunoreactivity for particular con-

Correspondence: Dr. Jun Yang, Department of Otorhinolaryngology-Head & Neck Surgery, Xinhua Hospital, Shanghai Jiaotong University School of Medicine, Shanghai Jiaotong University School of Medicine Ear Institute, Shanghai Key Laboratory of Translational Medicine on Ear and Nose diseases, Shanghai 200092, China.

Tel. +86.21.25078532 - Fax: +86.21.65156489.

E-mail: otology-xinhua@hotmail.com

Key words: Connexin 43, gap junction, development, cochlea, rat.

Contributions: WL, laboratory experiments, analysis interpretation and discussion of results, manuscript drafting; JY, research designed methods design. All the authors approved the final version to be published.

Funding: this study was supported by the National Natural Science Foundation of China (No. 81170919, No. 81470689), the project of Shanghai Municipal Science and Technology Commission (No. 14DJ1400201, No. 14DZ2260300).

Conflict of interest: the authors declare no potential conflict of interest.

Received for publication: 26 November 2014.

Accepted for publication: 3 February 2015.

This work is licensed under a Creative Commons Attribution NonCommercial 3.0 License (CC BY-NC 3.0).

©Copyright W.J. Liu and J. Yang, 2015

Licensee PAGEPress, Italy

European Journal of Histochemistry 2015; 59:2464

doi:10.4081/ejh.2015.2464

nexins in brain slices.<sup>16</sup> A previous study by Liu *et al.* also put forward similar views on Cx43 staining in cochlear tissue.<sup>5</sup>

Based on these points, the present study was designed to re-examine the immunolocalization of Cx43 in the rat cochlea. We successfully used transcatheter perfusion, fresh 4% paraformaldehyde, an ideal fixative for preserving cochlear morphology and protein immunoreactivity, cochlear post-fixation times of 30 min at room temperature, and short decalcification times for the optimal preservation of Cx43 immunogenicity. In the present study, Cx26 immunofluorescent staining was performed to confirm the reliability of our fixative protocol, and the results obtained agreed with previously reported expression patterns of Cx26.<sup>11</sup> We then re-examined the expression of Cx43 in the rat cochlea. Our results showed that Cx43 was specifically localized to the developing spiral ganglion neurons (SGNs) and their peripheral neurite projections to hair cells. To validate these findings, we performed double immunofluorescent labeling with antibodies for Cx43 and TUJ1 (beta III-tubulin), a marker in the mammalian cochlear nervous

system, by preferentially labeling all SGNs and their peripheral processes that innervated the hair cells.<sup>17</sup> To determine if there was colocalization between both proteins in these sites, cochlear cryostat sectioning was done on the same tissues over the same time points. Extensive colocalization of both proteins was observed in the region of the synaptic terminals at bases of inner hair cells (IHCs) and outer hair cells (OHCs) during post-natal 2 weeks and in developing and adult SGNs, confirming the specificity of Cx43 localization in this study. Moreover, quantitative real-time reverse transcription polymerase chain reaction (qRT-PCR) identified the expression of Cx43 in the modiolus at the mRNA level. The occurrence of Cx43 expression in the developing cochlear nervous tissues suggested the roles of Cx43 in early development of cochlear innervation, similar to that of the intercellular adhesive molecules such as N-cadherin -  $\beta$ -catenin complex that could promote neurite outgrowth, axonal guidance, and the generation and activity of synaptic junctions.<sup>18,19</sup>

## Materials and Methods

### Animals

Male and female Sprague-Dawley rats were used for this study at the following ages: newborn (P0), P1, P5, P8, P10, P14, P17, and adult (P28). All procedures in this study conformed to the regulations of the Animal Use and Care Committee of Shanghai Jiaotong University School of Medicine.

### Western blotting

Western blotting was performed using extracts from samples of the entire cochlea at P1. A whole brain was removed from one animal. Tissues obtained from the two different regions were homogenized separately in ice-cold RIPA Lysis Buffer (50 mM Tri-HCl, pH 7.6, 150 mM NaCl, 1% SDS, 1% Triton X-100, and 0.1 mM EGTA). Homogenates were fractionated by SDS-PAGE and electrophoretically transferred onto a nitrocellulose membrane. Membranes were blocked with non-fat dried milk and immunoblotting was performed using rabbit anti-Cx43 antibodies (1:400; Invitrogen, Carlsbad, CA, USA) and anti- $\beta$ -Actin monoclonal antibody (1:1000; Biyuntian, Hangzhou, China) served as an internal loading control. The protein bands were visualized by the application of horseradish peroxidase-conjugated secondary antibody, and were detected using a chemiluminescence reagent (Biyuntian). Reaction product levels were quantified by the Quantity One System (Bio-Rad, Hercules, CA, USA).

### Immunohistochemistry

Sprague-Dawley rats at various developmental stages were anesthetized by an intraperitoneal injection of 10% chloral hydrate (0.2 mL/100 g). Animals were perfused transcardially with normal saline and ice-cold 4% paraformaldehyde in 0.1M phosphate buffer (pH 7.4), and the cochleae were then quickly dissociated. The round and oval windows of the cochlea were opened, and a small hole made in the bony apex of the cochlea. After perilymphatic perfusion with the above fixative, the cochleae were post-fixed in the same fixative for 30 min at room temperature. P5 and older animals were decalcified in 10% EDTA at pH 7.4. Removal of excess tissue surrounding the cochlea every few hours, and shortening the decalcification time as much as possible, were critical for protecting immunoreactivity against potential loss during the decalcification procedures. The cochleae were thoroughly rinsed with 0.01M PBS and subsequently preserved in 15% sucrose for 3 h and in 30% sucrose overnight. Samples were then embedded in optimal cutting temperature compound (OCT Tissue-Tek® Compound; SakuraFinetek, Radnor, PA, USA) at 4°C for 3 h. The specimens were serially cut into 8  $\mu$ m sections using a Leitz cryostat microtome (Leitz, Grand Rapids, MI, USA). All sections were in a blocking/permeabilization solution [10% normal donkey serum (Jackson Labs, Bar Harbor, ME, USA) and 0.3% Triton X-100 in 0.01M PBS] for 30 min at room temperature, and then incubated at 4°C overnight with either mouse anti-Cx26 antibodies (1:250; Invitrogen) or with rabbit anti-Cx43 antibodies (1:150; Invitrogen) in 5% normal donkey serum and 0.1% Triton X-100 in 0.01M PBS. Immunofluorescent staining was performed using Cy2-conjugated donkey anti-rabbit antibodies (1:200; R&D, Minneapolis, MN, USA) or Alexa 546-conjugated donkey anti-mouse antibodies (1:400; Invitrogen) at 37°C for 1 h. For Cx43 and TUJ1 double labeling of consecutive mid-modiolus cryostat sections of the rat cochlea, prepared from P0-P28 rats, anti-Cx43 antibody was mixed with mouse anti-TUJ1 antibody (1:500; Covance, Princeton, NJ, USA), in PBS containing 0.1% Triton X-100 and 5% normal donkey serum, overnight at 4°C. Negative control sections were processed with PBS instead of the primary antibodies. After washing in PBS, the sections were incubated with Alexa 488-conjugated donkey anti-rabbit (1:200; Jackson Labs) and Alexa 546-conjugated donkey anti-mouse antibodies (1:400; Invitrogen) secondary antibodies. Sections were rinsed, counterstained with 4,6-diamidino-2-phenylindole (DAPI; Biyuntian) for 5 min, then fixed on coverslips with an anti-fade medium (Biyuntian). Images were photographed on a laser confocal scanning micro-

scopes (LSM 710, Zeiss, Jena, Germany) with a 40 $\times$  oil-immersion lens. Using Zeiss ZEN 2010 software, individual and merged immunofluorescence images were obtained. Images were processed using Adobe Photoshop software.

### RNA isolation and qRT-PCR

The cochlear modiolus mainly contains SGNs and nerve fibers, however, these fibers do not potentially contribute to RT-PCR results because of the absence of ribosomes in axons.<sup>20</sup> To investigate the existence of Cx43 mRNA in SGNs, we performed qRT-PCR on the modiolus tissue of the rat. Sprague-Dawley rats of P1, P8, and P14 (n=4 for each group) were rapidly decapitated and the cochlea exposed and placed in sterile double distilled water. The cochlea was then decapsulated, the membrane labyrinth further removed, and only the modiolus was collected. Total RNA extraction was performed using Trizol Reagent (Invitrogen) according to the manufacturer's recommendations. Reverse transcription was carried out using the RevertAid First Strand cDNA Synthesis Kit (Fermentas, Vilnius, Lithuania). PCR was subsequently performed with sense (Cx43: 5'-GCCTTTCGCTGTAACACTCAAC-3') and antisense (Cx43: 5'-CCTCTTCTTCTGTGTTAGCTTCTC-3') primers (Invitrogen) as follows: 95°C pre-denaturation (1 min), followed by 40 cycles at 95°C (15 s), 58°C (20 s), and 72°C (20 s), with a final extension at 72°C (5 min) and a melting curve analysis (72-95°C, increments of 1°C) to confirm primer specificity. Data were analyzed using the comparative threshold cycle (Ct) values ( $\Delta$ ACT) method, and the  $\beta$ -actin gene used as an endogenous internal control, at all stages. The threshold cycle (Ct) was normalized to the housekeeping gene *actin*, and the  $2^{-\Delta\Delta CT}$  method was used to calculate changes in gene expression.

### Statistical analyses

All the data were presented as the mean  $\pm$  standard error of mean (SEM). Comparisons of Cx43 mRNA levels among the various developmental stages were made using analysis of variance. When *F* ratios exceeded the critical value ( $P < 0.05$ ), the Tukey's test was used to compare P1 mean with each later developmental stage (P8, P14) mean.

## Results

### Antibody specificity

Western blotting analysis was performed to confirm the specificity of the polyclonal anti-Cx43 antibody used in the present study. A prominent band with a molecular weight of

approximately 43 kDa, corresponding to Cx43 protein, was detected in the whole rat cochlea of P1 and positive control rat brain (Figure 1). These findings demonstrated that this antibody was suitable for immunohistochemistry.

### Immunofluorescence detection and colocalization of Cx43 and TUJ1 in rat cochlear sections

To verify our fixative protocol, anti-Cx26 antibody was used for staining. Punctate labeling of Cx26 was detected in the basal cells in the *stria vascularis*, all fibrocytes of the spiral ligament, and between supporting cells in the organ of Corti (*data not shown*), consistent with a previous study.<sup>11</sup> This was the first evidence, based on immunofluorescent localization, that Cx43 was present in the neurite projections to the hair cell region, from birth to P14, where there was extensive colocalization between Cx43 and TUJ1 in double-labeling experiments. TUJ1, a specific marker of neural cells,<sup>21-23</sup> provided an excellent tool for the visualization of immature and mature type I and type II SGNs and their neurite projections associated with both IHCs and OHCs.<sup>17, 24-26</sup> The present study confirmed previous findings in the mammalian cochlea, that TUJ1 was strongly and exclusively expressed in the developing and mature SGNs and the afferent terminals below OHCs and IHCs. We extended these findings by demonstrating that the intra-ganglion spiral bundle (IGSB) in the rat, which represents the efferent system, showed positive immunoreactivity to TUJ1 throughout postnatal stages of development, while TUJ1 immunoreactivity had been observed in human intra-ganglion spiral bundle.<sup>27</sup> In addition, immunoreactivity for Cx43 and TUJ1 was colocalized in the IGSB (from P0 to P5) within the spiral ganglion. At P0, the earliest stage that we studied, a gradient of Cx43 expression levels in different cochlear turns was evident. The projection of TUJ1-positive afferent fibers into the organ of Corti also followed the same kind of gradients. At the apical turn, prominent Cx43 immunolabeling (in green) was uniformly distributed in the almost all SGNs, their distal neurites projecting to the lesser epithelial ridge, and the region of future IHCs. Similarly, TUJ1 (in red) showed strong labeling in the SGNs and the neurite projections to the IHC region. Merged images showed that virtually complete overlap (in yellow) of both fluorescence signals in the area mentioned, indicating colocalization of Cx43 and TUJ1 (Figure 2 A-I). No positive immunostaining was detected in the negative control (Figure 2 J-L). In the middle turn, in addition to Cx43-positive nerve terminals beneath the IHC, Cx43 immunoreactivity was first detected in the OHC region, coinciding perfectly with the first appearance of TUJ1 expression in the OHC region. SGNs

and IGSB were strongly positive to Cx43 and TUJ1, where colocalization of TUJ1 with Cx43 was also seen (Figure 3 A-I). In the basal turn, Cx43-immunopositive nerve terminals became well defined beneath IHCs and the three rows of OHCs, corresponding to the TUJ1-specific labeling of inner spiral plexus and outer spiral bundle, respectively. Merged images revealed Cx43 colocalized extensively with TUJ1 in the outer spiral bundle and inner spiral plexus, as well as most SGNs and IGSB (Figure 3 J-O). At P5, a gradient of expression vanished, both Cx43- and TUJ1-expressing outer spiral bundle at the base of OHCs became well defined with fibers reaching among the Deiters' cell in the apical turn, accompanied by stronger expression in the inner spiral plexus (Figure 4 A-I). No positive immunostaining was detected in the negative control (Figure 4 J-L). In the mid and basal region, Cx43- and TUJ1-labeled inner spiral plexus formed a calyceal-type innervation to the IHCs, and outer spiral bundles beneath all three rows of OHCs appeared cup-like, with almost all SGNs and IGSB being Cx43-positive. TUJ1 was perfectly colocalized in these sites (Figure 5 A-O). Because the gradient of expression was not observed at P5, the processing of our sections precluded analysis of apical and basal turn tissue at subsequent developmental stages, and we focused on the expression pattern of Cx43 in the mid turn of the cochlea. In the mid turn of P8 rat, we observed the absence of Cx43 immunoreactivity in the IGSB, and Cx43 immunolabeling was first detected in the interdental cells of the spiral limbus. Punctate Cx43 and TUJ1 immunolabeling was detected at the base of the OHCs. The inner spiral plexus labeling was more restricted to the basolateral region of the IHCs. Merged images showed a substantial overlap between the distribution of Cx43-positive and TUJ1-positive nerve terminals below the IHCs and OHCs (Figure 6 A-F). By P14, three parallel rows of Cx43- and TUJ1-positive outer spiral bundles extended from the base of the OHCs to the basilar membrane. The strong staining of the inner spiral plexus indicated innervation of the basolateral region of the IHCs. Double immunofluorescent staining exhibited Cx43 staining colocalizing nearly completely with TUJ1 staining in the inner spiral plexus and outer spiral bundles, and SGNs (Figure 6 G-L). From P14 onward, as shown for P17, regulation of Cx43 expression occurred. The inner spiral plexus and outer spiral bundles did not show any immunoreactivity for Cx43, as shown by the absence of colocalization of immunolabeling for Cx43 and TUJ1 in the synaptic region associated with the organ of Corti, but robust Cx43 immunolabeling remained in the SGNs. Type II fibrocytes of the spiral ligament and interdental cells maintained strong expression of Cx43 (Figure 7 A-I). In the adult, the overall

pattern of Cx43 immunostaining was similar to that found at P17, and Cx43 was still constrained to SGNs. Omission of primary antisera resulted in loss of these specific labeling profiles in adult cochlear tissues (Figure 8 E-F).

### Expression of Cx43 mRNA in microdissected modiolus by qRT-PCR analysis

There was different expression of Cx43 mRNA in the microdissected cochlear modiolus for the three age groups tested (one-way ANOVA,  $F=9.187$ ,  $P=0.007$ ) (Figure 9). There were significant differences between P8 compared with P1 (Tukey's test,  $P=0.009$ ) and P14 ( $P=0.017$ ). There was no significant difference in the expression of Cx43 mRNA between P1 and P14 ( $P=0.908$ ). Means and SEM of Cx43 mRNA at P8, P1, and P14 were  $4.024 \pm 0.860$ ,  $1.047 \pm 0.170$ , and  $1.367 \pm 0.323$ , respectively.

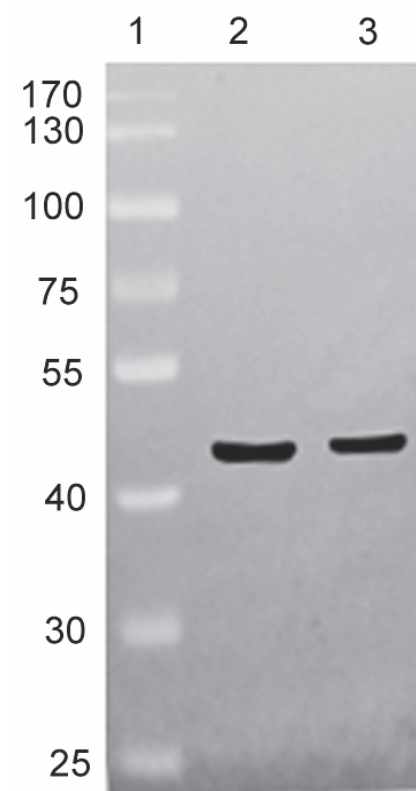
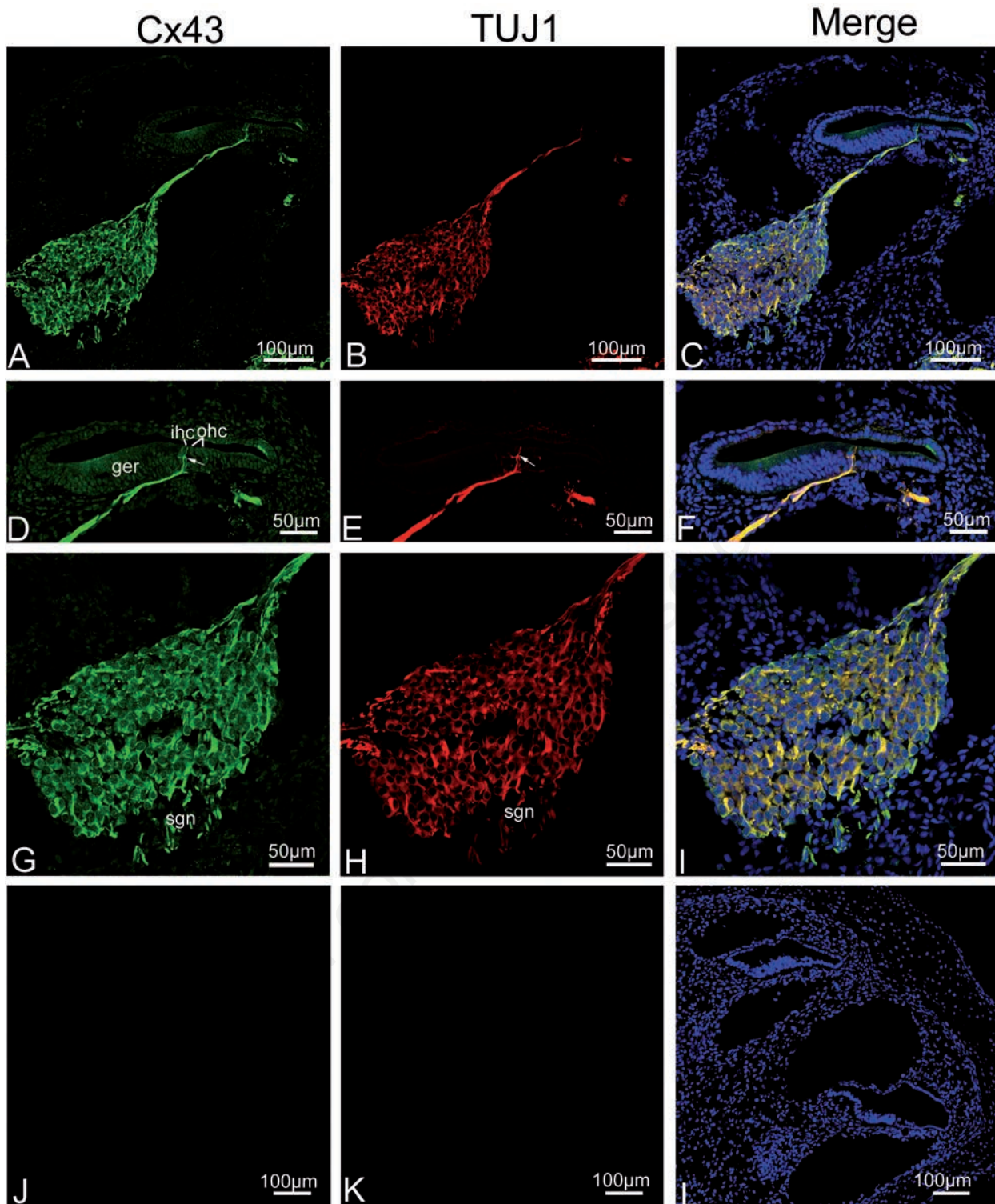
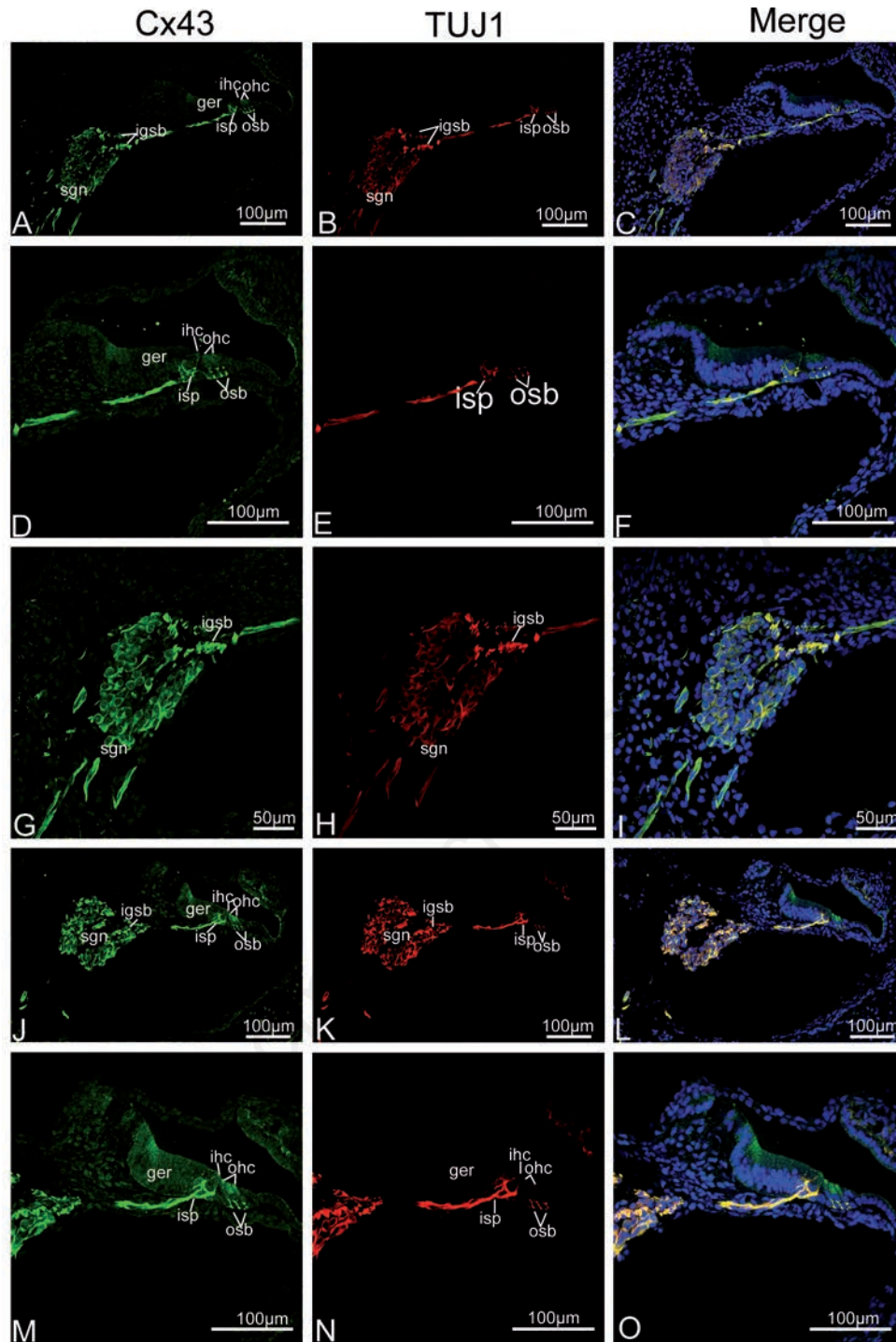


Figure 1. Western blotting assessment of the specificity of the anti-Cx43 polyclonal antibody. Lane 1 shows the molecular weight standards, lane 2 represents the positive control rat brain, showing a strong band at approximately 43 kDa, and lane 3 shows samples of cochlea from rats at P1 that also show a protein band at approximately 43 kDa.



**Figure 2.** Single plane confocal images of Cx43 (green) and TUJ1 (red) immunolabeling in the apical turn of the rat cochlea at P0 and the merged image + DAPI. A,B) An overview of Cx43 (green) and TUJ1 (red) labeling in the apical turn of the rat cochlea at P0; note that spiral ganglion neurons (sgns), and their neurites projecting toward the region of inner hair cells (ihcs) show significant immunoreactivity for Cx43 and TUJ1. C) There is extensive overlap between Cx43 and TUJ1 immunoreactivity in the sgn cell bodies and the afferent neurites as indicated by the yellow color in the merged image. D,E,F) Detail of Cx43 (green) and TUJ1 (red) expression in the organ of Corti in the apical turn and the merged image + DAPI. Cx43- and TUJ1-positive afferent fibers penetrated the basilar membrane and went towards the ihcs (arrow); note the region of outer hair cell (ohc) within the lesser epithelial ridge are devoid of Cx43 and TUJ1 immunolabeling; merged images showing complete overlap (yellow) of the two proteins in nerve fibers associated with the ihcs. G,H,I) Detail of Cx43 (green) and TUJ1 (red) expression in the sgn cell bodies in the apical turn and the merged image + DAPI; note that homogeneous Cx43 immunolabeling was observed in the sgn. J,K,L) The absence of Cx43 and TUJ1 immunofluorescence in negative control.



**Figure 3.** Single plane confocal images of Cx43 (green) and TUJ1 (red) immunolabeling in the mid and basal turn of the rat cochlea at P0 and the merged image +DAPI. A,B,C) An overview of Cx43 (green) and TUJ1 (red) labeling in the mid turn of the rat cochlea at P0 and the merged image +DAPI; Cx43 and TUJ1 immunolabeling was detected in the spiral ganglion neurons (sgns), their neurites innervating the inner (ihcs) and outer (ohcs) hair cells, and the intra-ganglion spiral bundle (igsb). D,E,F) Details of Cx43 and TUJ1 expression in the organ of Corti in the mid turn and the merged image +DAPI; Cx43- and TUJ1- labeled peripheral processes of the sgns extended into the ohcs, in addition to extensive Cx43- and TUJ1- labeled neurite terminals around the basolateral region of the ihcs. G,H,I) Detail of Cx43 (green) and TUJ1 (red) expression in the sgns in the mid turn and the merged image +DAPI; Cx43 overlapped completely virtually with TUJ1 in the igsb and sgns. J,K,L) An overview of Cx43 (green) and TUJ1 (red) labeling in the basal turn of the rat cochlea at P0 and the merged image +DAPI; note that Cx43 and TUJ1 immunolabeling is more pronounced in the synaptic regions underneath the ihcs than for the P0 mid cochlear tissue. Merged confocal images show the extensive overlap (yellow) of Cx43 and TUJ1 immunolabeling in the sgns, the peripheral neurites beneath the ihcs, the three rows of ohcs, and igsb. M,N,O) Details of Cx43 and TUJ1 expression in the organ of Corti in the basal turn and the merged image +DAPI; strong Cx43 immunolabeling was detected in the inner spiral plexus (isp) in the basolateral region of the ihcs, and outer spiral bundles (osb) beneath all three rows of the ohcs, as identified with TUJ1 labeling in double immunofluorescent labeling.

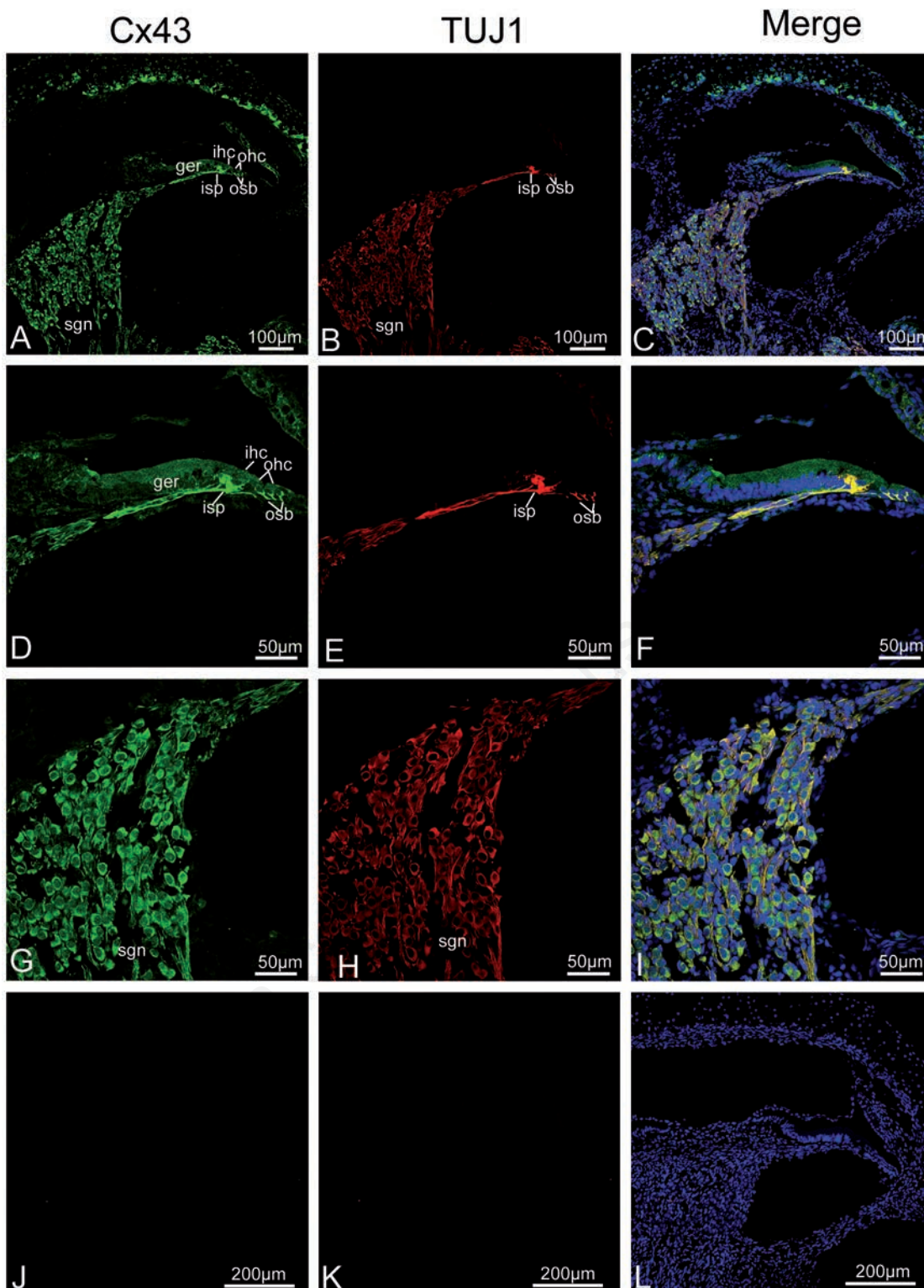
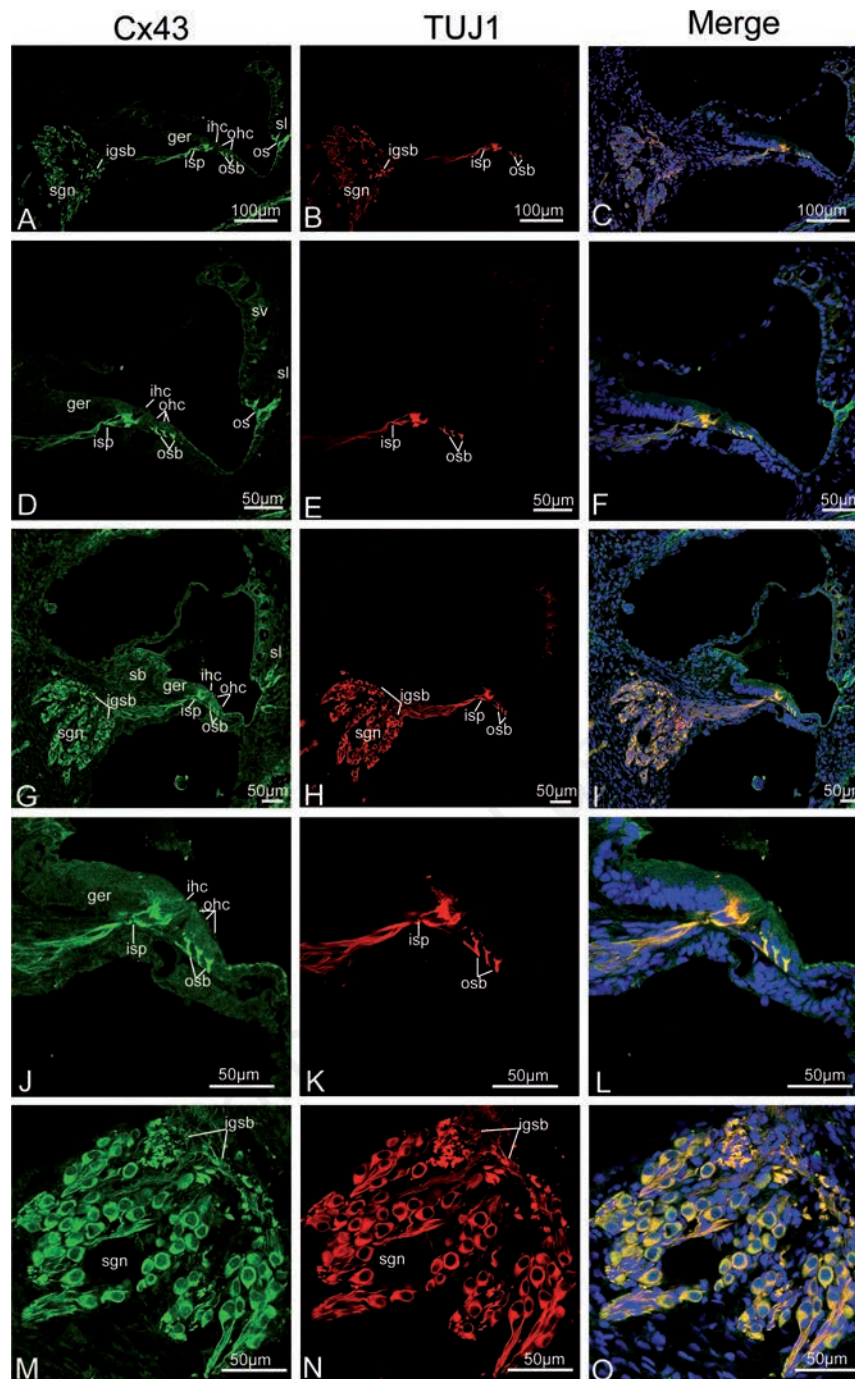
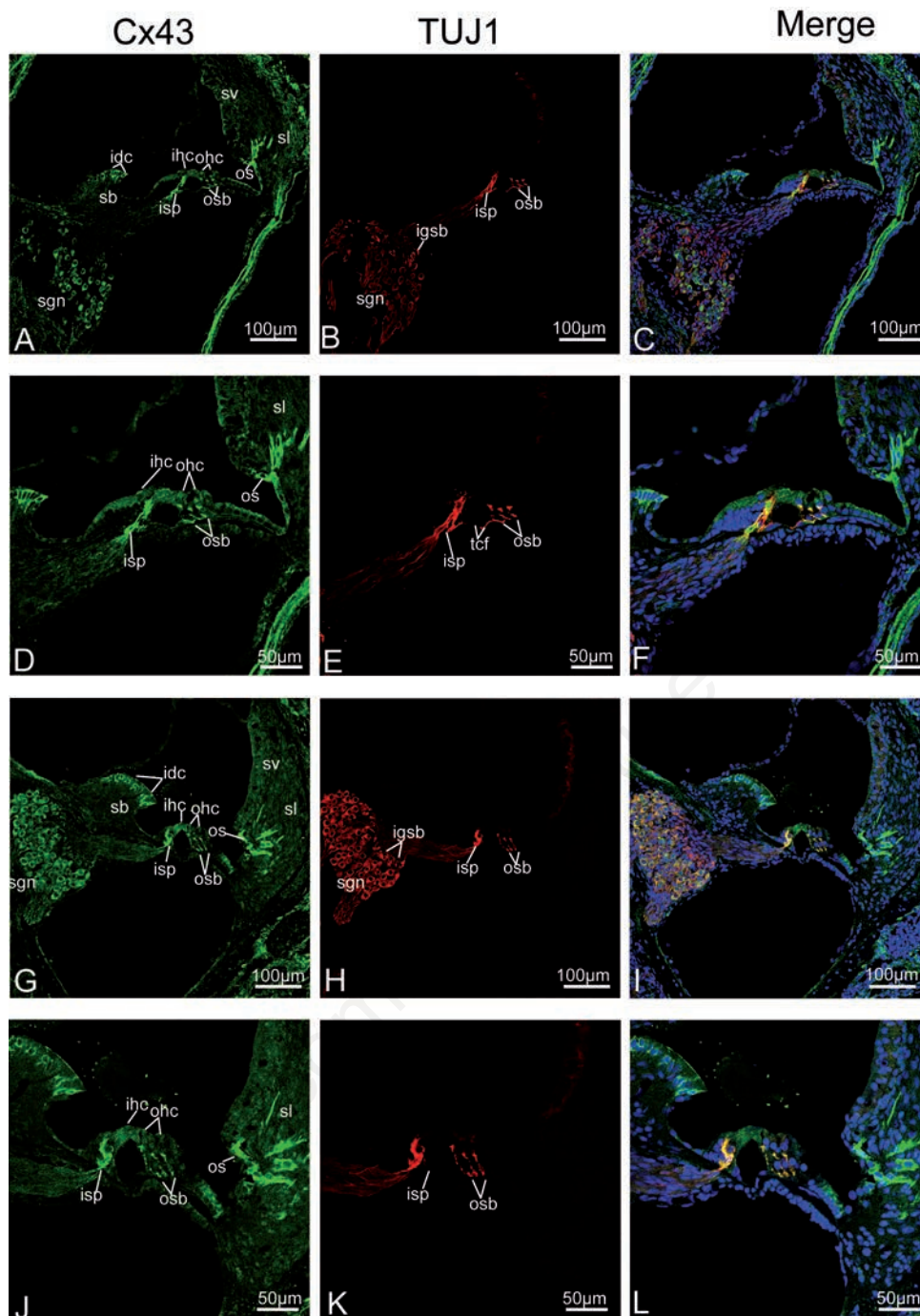


Figure 4. Single plane confocal images of Cx43 (green) and TUJ1 (red) immunolabeling in the apical turn of the rat cochlea at P5 and the merged image +DAPI. A,B,C) An overview of Cx43 (green) and TUJ1 (red) labeling in the apical turn of the rat cochlea at P5; Cx43 and TUJ1 immunolabeling was observed in the spiral ganglion neurons (sgns) and associated processes innervating both the inner (ihcs) and outer (ohcs) hair cells; merged confocal images showing a substantial overlap (yellow) between Cx43 and TUJ1 immunoreactivity in the inner spiral plexus (isp) below the ihc and outer spiral bundles (osb) below all three rows of ohc, sgns and their neurite. D,E,F) Details of Cx43 and TUJ1 expression in the organ of Corti in the apical turn and the merged image +DAPI; the Cx43- and TUJ1-labeled neurite terminals reach the ohc, and form a dense plexus beneath and surrounding the ihc; merged confocal images show the overlap (yellow) of Cx43 and TUJ1 immunolabeling in the isp and osb. G,H,I) Detail of Cx43 (green) and TUJ1 (red) expression in the sgns in the apical turn and the merged image +DAPI; Cx43 overlapped completely virtually with TUJ1 in the sgns. J,K,L) The absence of Cx43 and TUJ1 immunofluorescence in negative control. sl, spiral ligament; sv, *stria vascularis*; sb, spiral limbus.



**Figure 5.** Single plane confocal images of Cx43 (green) and TUJ1 (red) immunolabeling in the mid and basal turn of the rat cochlea at P5 and the merged image +DAPI. A,B,C) An overview of Cx43 (green) and TUJ1 (red) labeling in the mid turn of the rat cochlea at P5 and the merged image +DAPI; Cx43 and TUJ1 are strongly expressed in the spiral ganglion neurons (sgns), in the inner spiral plexus (isp), in the outer spiral bundles (osbs), and the intra-ganglion spiral bundle (igsb); note a few fibrocytes of the spiral ligament (sl) beneath the spiral prominence show Cx43 expression; merged confocal images show Cx43 overlapped exclusively with TUJ1 in the spiral ganglion neurons cell bodies and the igsb. D,E,F) Details of Cx43 and TUJ1 expression in the organ of Corti in the mid turn and the merged image +DAPI; the Cx43- and TUJ1-labeled calyceal-type neurite terminals are clearly detected around the basolateral region of the inner hair cell (ihc), and Cx43- and TUJ1-positive nerve terminals under the three rows of outer hair cell (ohc) exhibit a cup-like appearance; there is extensive overlap (yellow) between Cx43 staining and TUJ1 staining in the synaptic terminals beneath the ihc and ohc. G,H,I) An overview of Cx43 (green) and TUJ1 (red) labeling in the basal turn of the rat cochlea at P5 and the merged image +DAPI; the overall pattern of immunostaining was similar to that found in the mid turn of P5 rats; Cx43 and TUJ1 are still strongly expressed in the spiral ganglion neurons (sgn), in the inner spiral plexus (isp), in the outer spiral bundles (osb), and the intra-ganglion spiral bundle (igsb). J,K,L) Details of Cx43 and TUJ1 expression in the organ of Corti in the basal turn and the merged image +DAPI; robust labeling of Cx43- and TUJ1-positive terminals is found below the ihc and the ohc, and there was also extensive overlap (yellow) between Cx43 staining and TUJ1 staining in the synaptic terminals beneath the ihc and ohc. M,N,O) Detail of Cx43 (green) and TUJ1 (red) expression in the sgns in the basal turn and the merged image +DAPI; Cx43 overlapped completely virtually with TUJ1 in the igsb and sgns. sv, *stria vascularis*; sb, *stria basilaris*; os, outer sulcus cells.



**Figure 6.** Cx43 and TUJ1 immunolabeling and double labeling for Cx43 and TUJ1 in the mid turn of the rat cochlea at P8, P14 and the merged image +DAPI. A,B,C) An overview of Cx43 (green) and TUJ1 (red) labeling in the mid turn of the rat cochlea at P8 and the merged image +DAPI; Note that Cx43 immunolabeling is first present in the interstitial cells (idc) of the spiral limbus (sb), and disappears from the intra-ganglion spiral bundle (igsb), where only TUJ1 labeling is detected in the igsb, and no overlap between Cx43 and TUJ1 immunoreactivity is found; Cx43 immunoreactivity includes the spiral ganglion neurons (sgns), the inner spiral plexus (isp), and outer spiral bundles (osb), the idcs of the sb, and a few fibrocytes of the spiral ligament (sl). D,E,F) Details of Cx43 (green) and TUJ1 (red) expression in the organ of Corti in the mid turn of P8 rats and the merged image +DAPI; There is a substantial overlap (yellow) between the distribution of Cx43 and TUJ1 immunolabeling in the nerve terminals below the inner hair cells (ihcs) and the three rows of outer hair cells (ohcs), except for TUJ1-labeled tunnel crossing fibers (tcfs - shown in red), which cross the tunnel of Corti to contact the ohcs. G,H,I) An overview of Cx43 (green) and TUJ1 (red) labeling in the mid turn of the rat cochlea at P14; sgn and afferent terminals innervating the ihcs and ohcs (as identified with TUJ1 labeling) show pronounced Cx43 immunolabeling; Cx43 overlaps perfectly with TUJ1 in the sgn, the inner spiral plexus (isps) and outer spiral bundles (osbs). J,K,L) Details of Cx43 and TUJ1 expression in the organ of Corti in the mid turn of P14 rats and the merged image +DAPI; note that anti-Cx43- and anti-TUJ1 labeled three slender processes contacting both ohcs and Deiters' cells which approach the basilar membrane; merged confocal images showing a substantial overlap (yellow) of the expression of Cx43 and TUJ1 labeling below the ihcs and beneath the three rows of ohcs. sv, *stria vascularis*; os, outer sulcus cells; igsb, intra-ganglion spiral bundle.

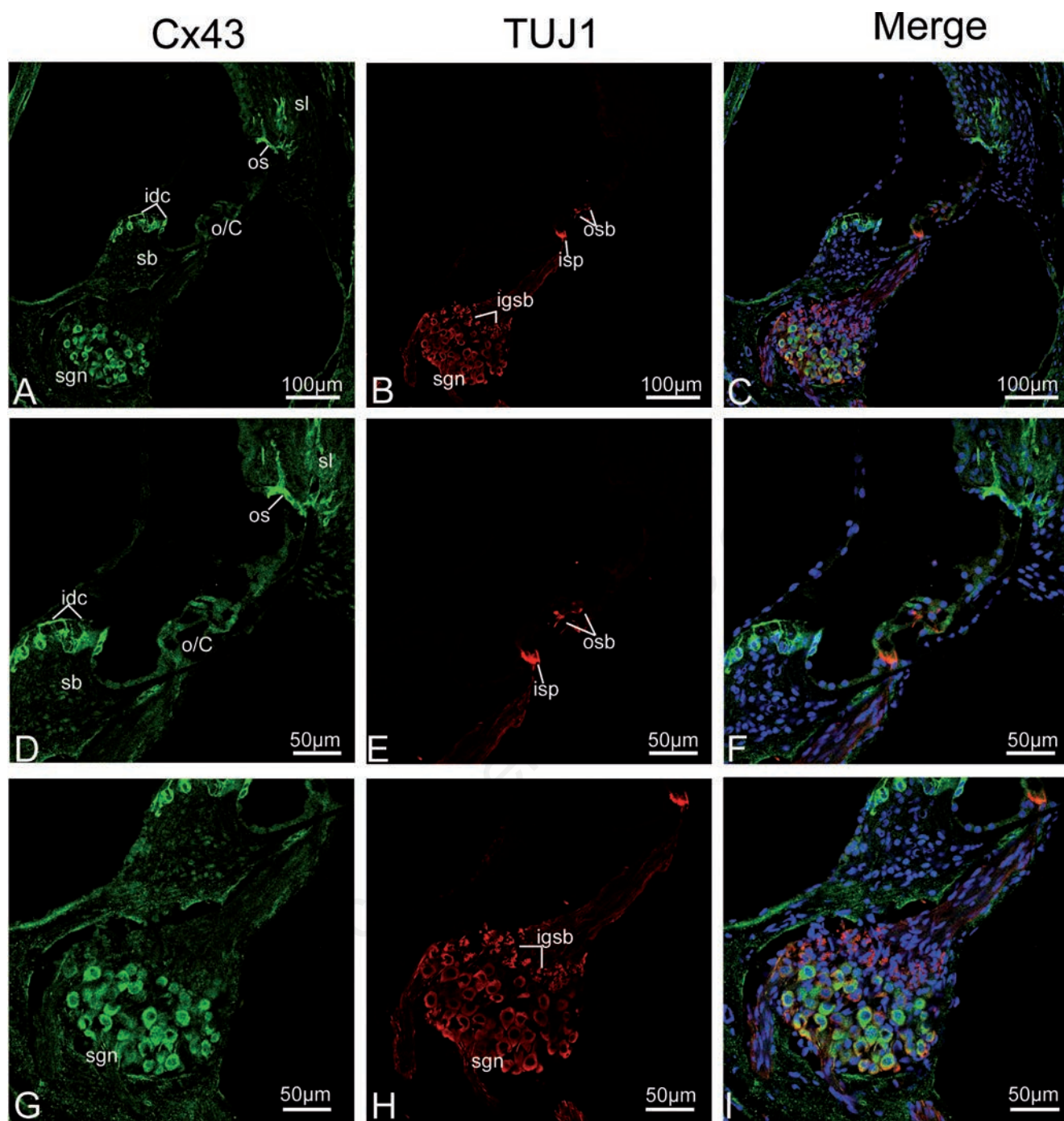


**Figure 7.** Cx43 and TUJ1 immunolabeling and double labeling for Cx43 and TUJ1 in the mid turn of the rat cochlea at P17 and the merged image +DAPI. A,B,C) An overview of Cx43 (green) and TUJ1 (red) labeling in the mid turn of the rat cochlea at P17 and the merged image +DAPI; Cx43 other than TUJ1 immunolabeling disappears from the inner spiral plexus (isp) and outer spiral bundles (osbs). D,E,F) Details of Cx43 and TUJ1 expression in the organ of Corti in the mid turn at P17 and the merged image +DAPI; the osb and isp are negative for Cx43, but are strongly positive for TUJ1. G,H I) Detail of Cx43 (green) and TUJ1 (red) expression in the spiral ganglion neurons (sgns) in the mid turn and the merged image +DAPI; positive Cx43 immunolabeling is observed in the sgns; this is reflected by a large amount of overlap between the distribution of Cx43 and TUJ1 in the sgns. sl, spiral ligament; sv, *stria vascularis*; sb, spiral limbus; os, outer sulcus cells; o/C, organ of Corti; igsb, intra-ganglion spiral bundle.

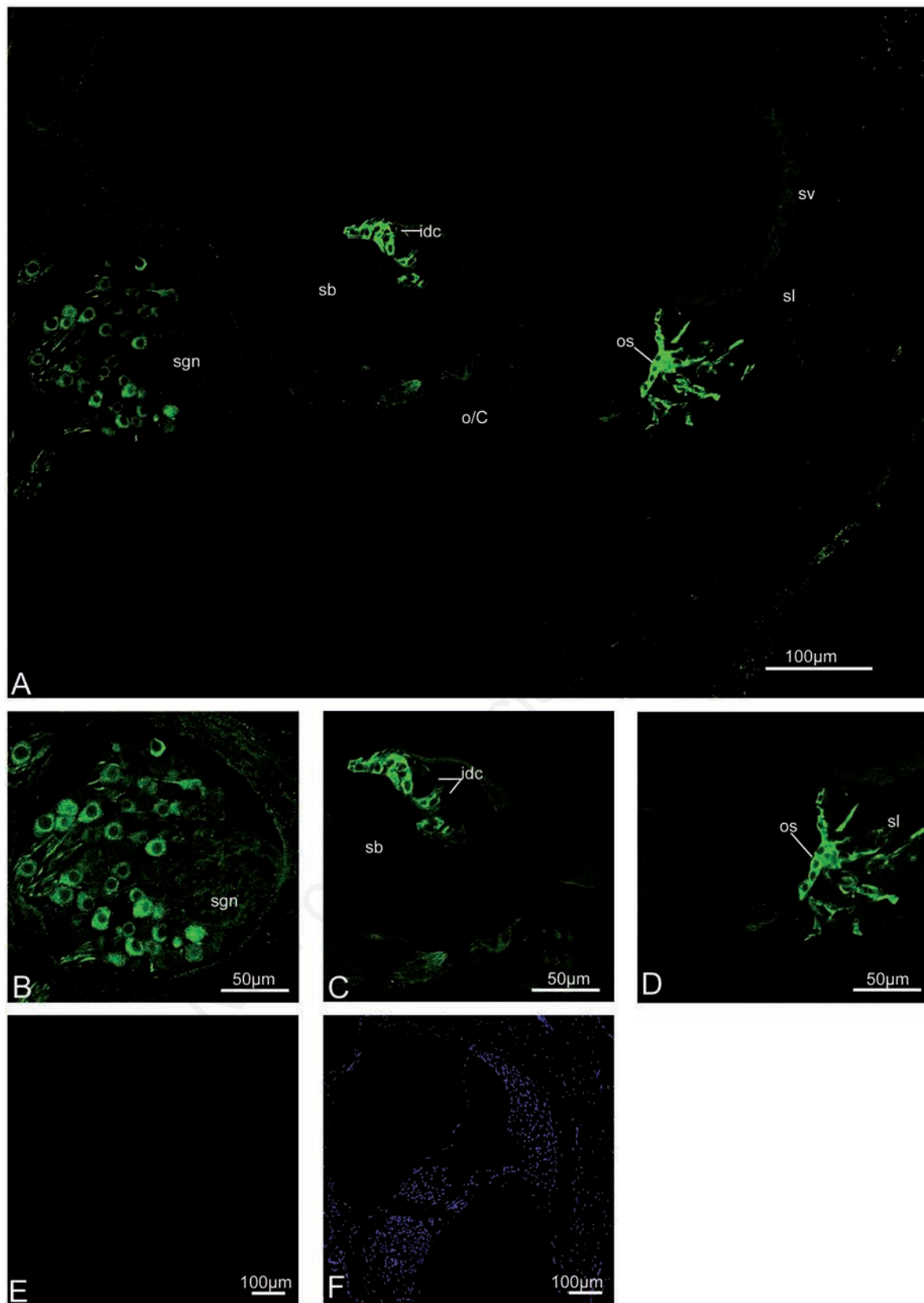


**Figure 8.** Cx43 immunolabeling in the adult rat cochlea. A) An overview of Cx43 labeling in the adult rat cochlea. Cx43 immunolabeling is still absent from the synaptic terminals beneath inner (ihcs) and outer (ohcs) hair cells. B,C,D) Details of Cx43 expression in the adult cochlea; The interdental cells (idc) of the spiral limbus (sb), the outer sulcus cell (os), a few fibrocytes of the spiral ligament (sl), and some spiral ganglion neurons (sgn) are positive for Cx43. E,F) Negative control for the adult cochlea with no primary antibodies. sl, spiral ligament; sv, *stria vascularis*; sb, spiral limbus; os, outer sulcus cells; sgn, spiral ganglion neuron; o/C, organ of Corti.

## Discussion

Gap junction proteins are widely distributed in the central and peripheral nervous system.<sup>28-32</sup> Ultrastructural analyses have identified connexins in GJs between peripheral nerves, such as nerve terminals of human dental pulp, skeletal muscle fibers in newborn rats, and in the rat sciatic nerve.<sup>33-35</sup> In this study, we demonstrated that Cx43 was specifically localized to peripheral neural circuitry of the rat cochlea during the first two post-natal weeks. It is in this period that the development and maturation of cochlear afferent innervation in the rat take place. At birth, type I and type II SGNs provide the afferent innervation of both hair cell types, respectively.<sup>36,37</sup> In the early post-natal period (P2-P11), prior to the onset of hearing, type I SGN afferent nerve fibers withdraw from the OHC, and their synapses condense at the IHC by neurite pruning, leading to individual IHC receiving exclusive punctate synapses from multiple type I SGNs, while type II SGN neurites retract from the IHC region and finally exclusively innervate the OHC *via* the outer spiral bundles.<sup>38,39</sup> We found that the early onset of Cx43 expression occurred in the developing SGNs and in their peripheral processes innervating the hair cells, and was sustained until P14. Double immunofluorescent staining showed TUJ1-labeled afferent terminals arising from type I and type II SGNs colocalized extensively with

Cx43 from P0 to P14, confirming the neural-specific Cx43 labeling in the rat cochlea, together with Cx43 mRNA expression in the SGNs, indicating that Cx43 expression in the rat cochlea followed the establishment of the developing afferent innervation to the sensory hair cells and thus contributed to this process. It was possible that Cx43 played a role in efferent synaptogenesis as well, as Cx43 immunolabeling was detectable in the IGSB between P0-P5, when efferent innervations to the hair cells undergo synaptic reorganizations.<sup>40</sup> The role of Cx43 in neurogenesis could be to provide an intercellular pathway for transmission of developmentally relevant molecules,<sup>29,41-44</sup> and a similar mechanism for Cx43 in cochlear synaptogenesis could be postulated.

Slightly after the onset of hearing (P17), there was a complete loss of Cx43 staining in all synaptic terminals, and the number of Cx43-immunopositive SGNs decreased. In addition, Cx43 mRNA expression in the SGNs of P14 was lower than that at P8 in parallel with the onset of hearing.<sup>45</sup> This change in the expression pattern of Cx43 strongly suggested that Cx43-containing GJs may play important roles in hearing for the auditory neurotransmission. Cx43 was detectable in the SGNs throughout postnatal development until the adult stage, suggesting that the target cells for hearing loss associated with mutations in Cx43 may be the SGNs. An outstanding feature of the distribution of Cx43 immunoreactivity in the SGNs was the uniform labeling through-

out the SGN cell bodies, rather than the characteristic punctate staining.<sup>41,46</sup> Coincidentally, a similar neuronal distribution of connexin proteins has been observed in the bat cochlear nucleus, in the SGNs of the human cochlea, and in the white matter of the brain stem.<sup>47-49</sup> Liu *et al.* proposed that non-plaque connexins may act as single channels or hemichannels.<sup>49</sup> This concept was supported by the ability of Cx43 to form hemichannels in non-junctional plasma membranes of some cells.<sup>50</sup> Since only morphological evidence is available for GJs or hemichannels composed of Cx43 in SGNs, additional studies should be conducted to further understand the role of these channels in the SGNs.

In addition to the neural expression pattern in the rat cochlea, we also found that stable expression of Cx43 in the interdental cells within the spiral limbus, consistent with its established role in mediating glucose transport in the spiral limbus of the rat cochlea.<sup>51</sup> The outer sulcus cell and a small number of fibrocytes of the spiral ligament also exhibited this stable expression, which implied it may be involved in cochlear homeostasis, possibly via the regulation of K<sup>+</sup> cycling to the cochlear endolymph.<sup>52,53</sup> We failed to detect Cx43 immunostaining in the organ of Corti, consistent with Cx43 mutant mice exhibiting a normal morphology of sensory hair cells and the presence of distortion product otoacoustic emissions (DPOAE) that closely related to the active process of OHCs.<sup>13,53</sup>

In conclusion, Cx43 was preferentially expressed in the developing afferent neurites and their synaptic contacts beneath the OHCs and IHCs. This neural predominant distribution occurred in a regulating pattern only during the first 2 post-natal weeks, coincident with the auditory development. However, the labeling of SGNs was sustained throughout the adult stage, though the results of qRT-PCR showed Cx43 mRNA differentially expressed in the modiolus. Our findings suggest a predominant role for Cx43 in cochlear synaptogenesis and auditory neurotransmission.

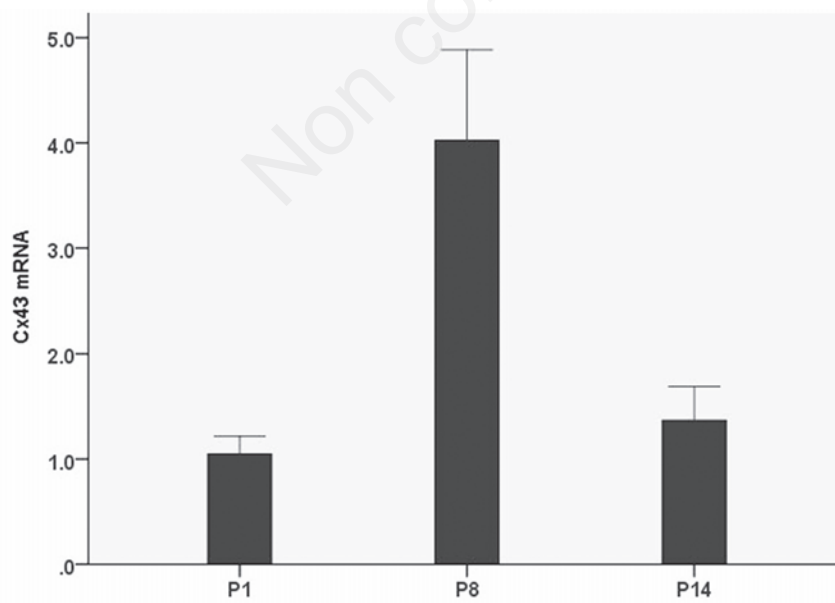


**Figure 9.** Developmental expression of Cx43 mRNA in microdissected specimens of the modiolus at three different post-natal developmental stages. Cx43 mRNA is present at the earliest post-natal time point examined (P1), and increases at P8 ( $P=0.009$ ). There is a decrease in Cx43 mRNA levels by P14 ( $P=0.017$ ). There were 4 rats in each group.

## References

1. Bennett MV, Barrio LC, Bargiello TA, Spray DC, Hertzberg E, Saez JC. Gap junctions: new tools, new answers, new questions. *Neuron* 1991;6:305-20.
2. Goodenough DA, Goliger JA, Paul DL. Connexins, connexons, and intercellular communication. *Ann Rev Biochem* 1996; 65:475-502.
3. Kelsell DP, Dunlop J, Stevens HP, Lench NJ, Liang JN, Parry G, et al. Connexin 26 mutations in hereditary non-syndromic

- sensorineural deafness. *Nature* 1997;387:80-3.
4. Grifa A, Wagner CA, D'Ambrosio L, Melchionda S, Bernardi F, Lopez-Bigas N, et al. Mutations in GJB6 cause nonsyndromic autosomal dominant deafness at DFNA3 locus. *Nat Genet* 1999;23:16-8.
  5. Liu XZ, Xia XJ, Adams J, Chen ZY, Welch KO, Tekin M, et al. Mutations in GJA1 (connexin 43) are associated with nonsyndromic autosomal recessive deafness. *Hum Mol Genet* 2001;10:2945-51.
  6. Zhao HB, Yu N. Distinct and gradient distributions of connexin26 and connexin30 in the cochlear sensory epithelium of guinea pigs. *J Comp Neurol* 2006;499:506-18.
  7. Majumder P, Crispino G, Rodriguez L, Ciubotaru CD, Anselmi F, Piazza V, et al. ATP-mediated cell-cell signaling in the organ of Corti: the role of connexin channels. *Purinergic Signal* 2010;6:167-87.
  8. Zhao HB, Yu N, Fleming CR. Gap junctional hemichannel-mediated ATP release and hearing controls in the inner ear. *Proc Natl Acad Sci USA* 2005;102:18724-9.
  9. Frenz CM, Van De Water TR. Immunolocalization of connexin 26 in the developing mouse cochlea. *Brain Res Brain Res Rev* 2000;32:172-80.
  10. Qu Y, Tang W, Zhou B, Ahmad S, Chang Q, Li X, et al. Early developmental expression of connexin26 in the cochlea contributes to its dominant functional role in the cochlear gap junctions. *Biochem Biophys Res Commun* 2012;417:245-50.
  11. Jagger DJ, Forge A. Compartmentalized and signal-selective gap junctional coupling in the hearing cochlea. *J Neurosci* 2006;26:1260-8.
  12. Cohen-Salmon M, Maxeiner S, Kruger O, Theis M, Willecke K, Petit C. Expression of the connexin43- and connexin45-encoding genes in the developing and mature mouse inner ear. *Cell and tissue research* 2004;316:15-22.
  13. Kim AH, Nahm E, Sollas A, Mattiace L, Rozental R. Connexin 43 and hearing: possible implications for retrocochlear auditory processing. *Laryngoscope* 2013;123:3185-93.
  14. Suzuki T, Takamatsu T, Oyamada M. Expression of gap junction protein connexin43 in the adult rat cochlea: comparison with connexin26. *J Histochem Cytochem* 2003;51:903-12.
  15. Nagy JI, Li X, Rempel J, Stelmack G, Patel D, Staines WA, et al. Connexin26 in adult rodent central nervous system: demonstration at astrocytic gap junctions and colocalization with connexin30 and connexin43. *J Comp Neurol* 2001;441:302-23.
  16. Nagy JI, Dudek FE, Rash JE. Update on connexins and gap junctions in neurons and glia in the mammalian nervous system. *Brain Res Brain Res Rev* 2004;47:191-215.
  17. Barclay M, Ryan AF, Housley GD. Type I vs type II spiral ganglion neurons exhibit differential survival and neuritogenesis during cochlear development. *Neural Dev* 2011;6:3-3.
  18. Uchida N, Honjo Y, Johnson KR, Wheelock MJ, Takeichi M. The catenin/cadherin adhesion system is localized in synaptic junctions bordering transmitter release zones. *J Cell Biol* 1996;135:767-79.
  19. Walsh FS, Doherty P. Neural cell adhesion molecules of the immunoglobulin superfamily: role in axon growth and guidance. *Annu Rev Cell Dev Biol* 1997;13:425-56.
  20. Oshima T, Ikeda K, Furukawa M, Takasaka T. Alternatively spliced isoforms of the Na<sup>+</sup>/Ca<sup>2+</sup> exchanger in the guinea pig cochlea. *Biochem Biophys Res Commun* 1997;233:737-41.
  21. Menezes JR, Luskin MB. Expression of neuron-specific tubulin defines a novel population in the proliferative layers of the developing telencephalon. *J Neurosci* 1994;14:5399-416.
  22. Zhang XM, Li Liu DT, Chiang SW, Choy KW, Pang CP, Lam DS, et al. Immunopanning purification and long-term culture of human retinal ganglion cells. *Mol Vis* 2010;16:2867-72.
  23. Si YC, Zhang JP, Xie CE, Zhang LJ, Jiang XN. Effects of Panax notoginseng saponins on proliferation and differentiation of rat hippocampal neural stem cells. *Am J Chin Med* 2011;39:999-1013.
  24. Lallemand F, Vandenbosch R, Hadjadj S, Bodson M, Breuskin I, Moonen G, et al. New insights into peripherin expression in cochlear neurons. *Neuroscience* 2007;150:212-22.
  25. Flores-Otero J, Davis RL. Synaptic proteins are tonotopically graded in postnatal and adult type I and type II spiral ganglion neurons. *J Comp Neurol* 2011;519:1455-75.
  26. Liu W, Kinnefors A, Bostrom M, Edin F, Rask-Andersen H. Distribution of pejkakin in human spiral ganglion: an immunohistochemical study. *Cochlear Implants Int* 2013;14:225-31.
  27. Liu W, Bostrom M, Kinnefors A, Linthicum F, Rask-Andersen H. Expression of myelin basic protein in the human auditory nerve - an immunohistochemical and comparative study. *Auris Nasus Larynx* 2012;39:18-24.
  28. Miragall F, Simburger E, Dermietzel R. Mitral and tufted cells of the mouse olfactory bulb possess gap junctions and express connexin43 mRNA. *Neurosci Lett* 1996;216:199-202.
  29. Rozental R, Srinivas M, Gokhan S, Urban M, Dermietzel R, Kessler JA, et al. Temporal expression of neuronal connexins during hippocampal ontogeny. *Brain Res Brain Res Rev* 2000;32:57-71.
  30. Chang Q, Balice-Gordon RJ. Gap junctional communication among developing and injured motor neurons. *Br Brain Res Brain Res Rev* 2000;32:242-9.
  31. Yoshimura T, Satake M, Kobayashi T. Connexin43 is another gap junction protein in the peripheral nervous system. *J Neurochem* 1996;67:1252-8.
  32. Fulton BP. Gap junctions in the developing nervous system. *Perspect Dev Neurobiol* 1995;2:327-34.
  33. Schmalbruch H. Skeletal muscle fibers of newborn rats are coupled by gap junctions. *Dev Biol* 1982;91:485-90.
  34. Koling A, Rask-Andersen H. Membrane junctions in the subodontoblastic region. A freeze-fracture study of the human dental pulp. *Acta Odontol Scand* 1983;41:99-109.
  35. Li X, Lynn BD, Olson C, Meier C, Davidson KG, Yasumura T, et al. Connexin29 expression, immunocytochemistry and freeze-fracture replica immunogold labelling (FRIL) in sciatic nerve. *Eur J Neurosci* 2002;16:795-806.
  36. Echter SM. Developmental segregation in the afferent projections to mammalian auditory hair cells. *Proc Natl Acad Sci USA* 1992;89:6324-7.
  37. Yang T, Kersigo J, Jahan I, Pan N, Fritzsche B. The molecular basis of making spiral ganglion neurons and connecting them to hair cells of the organ of Corti. *Hear Res* 2011;278:21-33.
  38. Rubel EW, Fritzsche B. Auditory system development: primary auditory neurons and their targets. *Annu Rev Neurosci* 2002;25:51-101.
  39. Bulankina AV, Moser T. Neural circuit development in the mammalian cochlea. *Physiology (Bethesda)* 2012;27:100-12.
  40. Rontal DA, Echter SM. Developmental segregation in the efferent projections to auditory hair cells in the gerbil. *J Comp Neurol* 2003;467:509-20.
  41. Leung DS, Unsicker K, Reuss B. Expression and developmental regulation of gap junction connexins cx26, cx32, cx43 and cx45 in the rat midbrain-floor. *Int J Dev Neurosci* 2002;20:63-75.
  42. Montoro RJ, Yuste R. Gap junctions in developing neocortex: a review. *Brain Res Brain Res Revs* 2004;47:216-26.
  43. Sutor B. Gap junctions and their implications for neurogenesis and maturation of synaptic circuitry in the developing neocortex. *Results Probl Cell Diff* 2002;39:53-73.
  44. Sutor B, Hagerty T. Involvement of gap junctions in the development of the neocortex. *Biochim Biophys Acta* 2005;1719:59-68.
  45. Geal-Dor M, Freeman S, Li G, Sohmer H.

- Development of hearing in neonatal rats: air and bone conducted ABR thresholds. *Hear Res* 1993;69:236-42.
46. Chen MJ, Kress B, Han X, Moll K, Peng W, Ji RR, et al. Astrocytic CX43 hemichannels and gap junctions play a crucial role in development of chronic neuropathic pain following spinal cord injury. *Glia* 2012;60:1660-70.
47. Dermietzel R, Traub O, Hwang TK, Beyer E, Bennett MV, Spray DC, et al. Differential expression of three gap junction proteins in developing and mature brain tissues. *Proc Natl Acad Sci USA* 1989;86:10148-52.
48. Horowitz SS, Stamper SA, Simmons JA. Neuronal connexin expression in the cochlear nucleus of big brown bats. *Brain Res* 2008;1197:76-84.
49. Liu W, Bostrom M, Kinnefors A, Rask-Andersen H. Unique expression of connexins in the human cochlea. *Hear Res* 2009;250:55-62.
50. Li H, Liu TF, Lazrak A, Peracchia C, Goldberg GS, Lampe PD, et al. Properties and regulation of gap junctional hemichannels in the plasma membranes of cultured cells. *J Cell Biol* 1996;134:1019-30.
51. Matsunami T, Suzuki T, Hisa Y, Takata K, Takamatsu T, Oyamada M. Gap junctions mediate glucose transport between GLUT1-positive and -negative cells in the spiral limbus of the rat cochlea. *Cell Commun Adhes* 2006;13:93-102.
52. Spicer SS, Thomopoulos GN, Schulte BA. Structural evidence for ion transport and tectorial membrane maintenance in the gerbil limbus. *Hear Res* 2000;143:147-61.
53. Wangemann P. K<sup>+</sup> cycling and the endocochlear potential. *Hear Res* 2002;165:1-9.

Non commercial use only